Atmos. Chem. Phys. Discuss., 11, 26143–26171, 2011
www.atmos-chem-phys-discuss.net/11/26143/2011/
doi:10.5194/acpd-11-26143-2011

Atmospheric Chemistry and Physics Discussions

Effect of bacterial ice nuclei on the frequency and intensity of lightning activity inferred by the BRAMS model

F. L. T. Gonçalves[1], J. A. Martins[2], R. I. Albrecht[3], C. A. Morales[1], M. A. Silva Dias[1], and C. E. Morris[4]

[1]Dept. of Atmospheric Sciences, IAG/USP/Brazil, Rua do Matão 1226, 05508090, São Paulo , SP, Brazil
[2]Universidade Tecnológica Federal do Paraná, 86036-370, Londrina, PR, Brazil
[3]DSA/CPTEC, Instituto Nacional de Pesquisas Espaciais, Cachoeira Paulista, SP, Brazil
[4]INRA, UR407 Pathologie Végétale, 84140 Montfavet, France

Received: 20 April 2011 – Accepted: 29 August 2011 – Published: 21 September 2011

Correspondence to: F. L. T. Gonçalves (fgoncalv@model.iag.usp.br)

Published by Copernicus Publications on behalf of the European Geosciences Union.

Abstract

Many studies from the last decades have shown that airborne microorganisms can be intrinsically related with atmospheric processes. Certain bacteria may constitute the most active ice nuclei found in the atmosphere and might have some influence on the formation of ice crystals in clouds. This study deals with the ice nucleation activity of *Pseudomonas syringae* inside of thunderstorms through numerical simulations using BRAMS (*Brazilian Regional Atmospheric Model System*). The numerical simulations were developed in order to investigate the effect on the total amount of rainwater as a function of ice nuclei (IN) *P. syringae* concentrations with different scenarios (classified as S2 to S4 scenarios) corresponding to maximum 10^2 to 10^3 IN bacteria per liter of cloud water plus the RAMS default (classified as S5 scenario). Additionally, two other scenarios were included without any IN (S1) and the sum of RAMS default and S4 scenario (classified as S6). The chosen radiosonde data is for 3 March 2003, typical summertime in São Paulo City which presents a strong convective cell. The objective of the simulations was to analyze the effect of the IN concentrations on the BRAMS modeled cloud properties and precipitation. The simulated electrification of the cloud permitted analysis of the total flashes estimated from precipitable and non-precipitable ice mass fluxes. Among all scenarios, only S4 and S6 presented a tendency to decrease the total cloud water, and all bacteria scenarios presented a tendency to decrease the total amount of rain at the ground (−8 %), agreeing with literature. All bacteria scenarios also present higher precipitable ice concentrations compared to S5 scenario, the RAMS default. The main results present the total flash number per simulation as well. From the results, the total flash number, in the simulation S4 and S6, is twice higher than the RAMS default. Even the smaller bacteria concentrations (scenarios S2 and S3) produced higher number of flashes, 4 to 5, compared to the S5 with only 3. This result is a function of the hydrometeors in each simulation. In conclusion, IN bacteria could affect directly the thunderstorm structure and lightning formation with many other microphysical implications.

ACPD

11, 26143–26171, 2011

1 Introduction

Over the past several years there has been a surge in novel research concerning the interaction of airborne microorganisms with atmospheric processes. There is growing evidence that bacteria and fungi, in particular, can influence atmospheric chemistry via the release of carbon and ions into the atmosphere (Elbert et al., 2007) and chemical transformation of atmospheric carbon sources (Deguillaume et al., 2008). Certain bacteria are also the most active ice nuclei found in the atmosphere and might have some influence on the formation of ice crystals in clouds (Möhler et al., 2007; Morris et al., 2004). Environmental sampling revealed that ice nucleation-active (INA) strains of the bacterium *Pseudomonas syringae* were enriched in rain and snowfall compared to other environmental sources where this bacterium is found (plants, water, epilithic biofilms) (Morris et al., 2008). In an experimental cloud chamber, this and other species of INA bacteria could induce condensation and subsequent freezing of cloud droplets (Möhler et al., 2008). Efforts to model the impact of INA microorganisms on the physical processes in clouds leading to precipitation have yielded somewhat conflicting results. Recent work by Hoose et al. (2010) in particular suggests that primary biological aerosol particles in general have only a minor impact on cloud glaciation on a global scale relative to other heterogeneous ice nuclei in the atmosphere.

Microbiological as well as atmospheric physics approaches have suggested that certain types of plant-associated bacteria (such as *P. syringae*) and fungi (such as ice nucleation active *Fusarium* spp. (Pouler et al., 1992), in the atmosphere could be important for rainfall formation (Morris et al., 2004; Bauer et al., 2003; Szyrmer and Zawadzki, 1997). The authors came to this conclusion because these bacteria produce a protein on their outer membrane that is one of the most active of the naturally-occurring ice nuclei (compounds capable of catalyzing the freezing of water – Jaenicke, 2005), and because freezing of cloud water is a critical step for rainfall over major parts of the earth (Sattler et al., 2002; Ariya and Amyot, 2004; Diehl et al., 2000; Hamilton and Lenton, 1998). These micro-organisms are widely distributed across the planet, multiply readily, survive airborne dissemination up to the clouds and fall out with precipitation. If they

Discussion Paper | Discussion Paper | Discussion Paper | Discussion Paper |

ACPD
11, 26143–26171, 2011

Effect of bacterial ice nuclei on lightning activity inferred by BRAMS

F. L. T. Gonçalves et al.

play a catalyzing role in the formation of precipitation, they could have applications in drought mitigation.

According to Amato et al. (2005), the total bacterial density in clouds is about 3×10^4 cells m^{-3} of cloud volume (1×10^5 cells ml^{-1} of cloud water) based on direct visual counts of total cells. Most of the isolated micro-organisms, including 12 fungal and 17 bacterial strains, were described for the first time in atmospheric water by Amato and colleagues. Amato et al. (2007) found bacteria mainly in the genera *Pseudomonas, Sphingomonas, Staphylococcus, Streptomyces,* and *Arthrobacter* and fungi such as *Cladosporium* or *Trametes*. Additionally, Phillips et al. (2009) have shown in preliminary simulations, performed for a case of deep convection over Oklahoma, that certain concentrations of ice nuclei with activities similar to bacterial ice nuclei could influence significantly: (1) the average number and size of ice crystals in the clouds; (2) the horizontal cloud coverage in the free troposphere; and (3) precipitation and incident solar insolation at the surface, which influence rates of bacterial growth. There is currently very little data on the atmospheric concentration of biological ice nuclei. Approximations of the concentration of *P. syringae*, which seems to be the most frequently encountered and most active of the biological ice nuclei, can be made from ecological studies of its abundance in freshly fallen snow. The maximum concentration of P. syringae, observed in fresh snow fall, is 10^5 bacteria l^{-1} (Morris et al., 2008). All strains of *P. syringae* isolated from snow fall to date have measurable ice nucleation activity (Morris et al., 2008). Based on the reported ice nucleation activities in these samples (Morris et al., 2008) and the cumulative frequency profile of the most active ice nucleation active strain reported to date (Orser et al., 1985), about 10 % of the cells of *P. syringae* would be active at $-8\,^{\circ}$C and nearly all of the cells would be active at $-12\,^{\circ}$C. Direct observations of biological ice nuclei in freshly fallen snow fall have revealed at most 200 ice nuclei l^{-1} of melt water active at $-7\,^{\circ}$C (Christner et al., 2008). The snow analyzed in these studies might have accumulated ice nuclei from the atmosphere as it fells. Nevertheless, these values provide a realistic range of numbers of biological ice nuclei per volume of cloud water.

ACPD
11, 26143–26171, 2011

Phillips et al. (2009) also wrote that the abundance of bacterial ice nuclei in the environment, their capacity to induce ice formation and their overall apparent link to the water cycle lead to the open question of whether emissions of such ice nucleating biogenic particles from their sources (plants in particular) can be modified by their own effects on clouds and atmospheric conditions, forming a weak feedback system, which is consistent with the proposal of Sands et al. (1982). If there is such a feedback system, there is also emerging evidence that it might have an impact on bacterial evolution in addition to an impact on atmospheric processes. In particular, results of a recent population genetics study suggest that ice nucleation activity is a driver for the evolution of plant pathogenicity in *P. syringae* (Morris et al., 2010). Elucidating the roles that ice nucleation can play in processes of the physical environment is therefore stimulating new directions of investigation on the subsequent impact of ice nucleation activity on the biology and evolution of microorganisms with this capacity. Levin et al. (2005) show simulations without ice-nucleating ability of the mineral dust, but allowing the soluble component of the mixed aerosols to act as efficient giant cloud condensation nuclei (CCN), enhances the development of the warm rain. In their simulations the rain amounts increased by as much as 37 % compared to the case without giant CCN. On the other hand, allowing the mineral dust particles to also act as efficient ice nuclei (IN) reduces the amount of rain on the ground compared to the case when they are inactive. Their simulations reveal when the dust particles are active as both giant CCN and effective IN, the continental clouds become wider.

One important role of ice formation in environmental processes is in the production of lightning. The main mechanism responsible for cloud electrification is the non-inductive mechanism, which involves rebounding collisions between graupel and ice crystals in the presence of supercooled liquid water (MacGorman and Rust, 1998). During the rebounding collisions, electric charge is transferred between the particles with opposite signs. The amount of charge transferred depends on the particles sizes and their fall velocity, while the sign depends on the cloud temperature and supercooled liquid water content (e.g. Takahashi, 1978; Saunders et al., 1991, 2006; Pereyra et al., 2000;

ACPD
11, 26143–26171, 2011

Takahashi and Miyawaki, 2002). Due to gravitational force the smaller particles are carried aloft into higher regions of the cloud by its updrafts, creating electrical charged centers inside the cloud. When the electrical potential differences between these centers are strong enough to break up the dielectric breakdown of air, lightning is initiated. As bacterial ice nuclei in the environment could lead to an increased number of ice crystals, an increase in the number of rebounding collisions between ice particles would be observed, increasing the total amount of electrical charge transferred and the charged centers, which in turn increases lightning activity in the cloud.

Furthermore, the impact of biological particles on clouds extends beyond potentially affecting precipitation alone. Impacts on the phase of clouds and on precipitation feed into the global energy and water cycle. This alone is motivation for understanding the role of biological aerosols (Morris et al., 2011). Numerical modeling plays an important role in understanding these processes.

The impact on cloud electricity is also extended beyond the number of lightning discharges alone. Lightning is the largest non-anthropogenic source of NO_2 and NO (together referred as NO_x) in the free troposphere. NO_x is an important trace gas in ozone chemistry and an increase in lightning frequency could increase lightning-generated NO_x in the middle and upper troposphere, and as well as the ozone concentrations. Ozone is the third most important greenhouse gas, playing a big role in the radiative climate forcing that could be affected by changes in lightning production.

In this investigation, we used a high-resolution configuration of the Brazilian Regional Atmospheric Modeling System (BRAMS). The RAMS model utilizes the full set of non-hydrostatic, Reynolds-averaged primitive equations (Tripoli and Cotton, 1982). The Brazilian version of the RAMS is the result of changes incorporated by Brazilian users in recent years, which include a simple photochemical and a soil moisture scheme. Validation of the BRAMS for use in Amazon region simulations is presented by Freitas et al. (2009). The cloud microphysics in BRAMS is described by Martins et al. (2009) based on Walko et al. (1995) and Meyers et al. (1992, 1997).

ACPD
11, 26143–26171, 2011

2 Methodology

2.1 RAMS model and ice nucleation

The numerical simulations were developed in order to investigate the effect of IN concentrations on the total amount of rainwater in the integrated vertical column and on rainfall. Homogeneous initializations were performed and simulations carried out for a time interval of 3 h, Heating and wetting at the center of the grid were introduced after 10 min of simulation, mimicking a low level forcing in order to develop a convective cell. This low level forcing was applied according to Gonçalves et al. (2008). The chosen temperature and humidity profiles to initiate the model were taken from a radiosonde on 3 March 2003, which is typical for summertime at São Paulo City (−43.66° longitude, −23.59° latitude) (Fig. 1a). Figure 1b shows the radiosonde of the date 3 March. Figure 1c presents the radar image of the event at 18:00 GMT, emphasizing a strong convective event exactly over São Paulo City. With the purpose of testing the sensitivity of microphysical parameters, the low level forcing was activated without topography, wind and surface characteristics to emphasize the cloud microphysical aspects. The objective of the simulations is to analyze the effect of the IN concentrations on the BRAMS modeled cloud properties, precipitation and lightning activity. Lightning frequency was inferred by the frozen particles fluxes described in the next section (Sect. 2.2).

The simulated low level forcing was based on Walko et al. (1995) and was designed to produce complete development of both liquid and ice phases. The computational domain involved a zone 20 km deep and 60 km wide. The adopted horizontal grid spacing was 500 m and the vertical one was variable. A Rayleigh friction absorbing layer was used in the top of the model to prevent the reflection of gravity waves. The configuration of additional microphysical parameters in the numerical simulations was adjusted according to values suggested in empirical studies. Two other important parameters that directly impacted IN were the CCN concentration and the shape of the frequency distribution of their sizes. Previous studies have shown that the precipitation process is strongly affected by CCN concentrations changes (Martins et al., 2009) and also the

ACPD
11, 26143–26171, 2011

shape parameter of the size distributions. In addition, the two parameters were related to each other (Martins and Silva Dias, 2009). Higher shape parameter decreased the spectral width of hydrometeor categories, including pristine ice. Although the numerical simulations were sensitive to specified microphysical parameters, it is assumed a CCN concentration of 300 cm^{-3} and the shape parameter was set to 2, which corresponds to relatively clear atmospheric conditions (Gonçalves et al., 2008).

Based on the model characteristics described above, six numerical experiments were run in order to analyze the effects of IN concentrations on modeled cloud properties, precipitation and electrification. These simulations considered a series of ice nucleation parameterizations as shown in Fig. 2. In the first numerical experiment (S1) the model was run in the homogeneous nucleating mode only. In this case, a small group of water molecules take on a crystal lattice structure due to random motions. After the initial crystal structure was established, it grew throughout the entire water droplet. The homogeneous nucleation followed the parameterization proposed by DeMott et al. (1994) and was applied in the temperature range from −50 °C to −30 °C (the value at −50 °C was then applied to colder temperatures). In the second numerical experiment (S3 scenario), homogeneous nucleation occurred and IN concentration was assumed to follow 100 000 times less the total population of bacteria (*P. syringae*), a fraction of Amato et al. (2005) work, where temperature range of −12 °C to −2 °C. Only a fraction of total bacteria can act as INA (Morris et al., 2008), therefore it was set 1000 INA per l of cloud water (see Fig. 2, for S3 scenario). As no observational data were available at temperatures colder than −12 °C, the IN concentration for −10 °C was used, as illustrated in Fig. 2. Therefore, the number of nucleated ice crystals at a certain time (t) was also based on Morris et al. (2008). The *P. syringae* IN concentrations were assumed homogeneous over the whole model domain at the beginning of the simulation ($t = 0$) with no changes after the simulation started, there is no depletion of IN. All bacteria, in these scenarios, induced ice formation, as indicated in Fig. 2.

ACPD
11, 26143–26171, 2011

The third and fourth numerical experiments were the same as S2, but the initial IN concentration profiles were 10 (S3) and 100 (S4) times the value of S2. The last numerical scenario (S5) is the one that represents RAMS' default parameterization, and it includes a variety of physical mechanisms: homogeneous nucleation (as in scenario S1); deposition nucleation and condensation-freezing nucleation (Meyers et al., 1992); contact freezing nucleation (Cotton et al., 1986). The sets of nucleation parameterization characteristics described above for each simulation are summarized in Table 1. S6 presents IN concentration summing up the S5 (RAMS default) and S4 scenario. Secondary ice production, based on the Hallett-Mossop theory (Cotton et al., 1986), is included in all scenarios. *P. syringae* bacterial concentrations are based on Amato et al. (2005, 2007), where we adjusted a polynomial equation to the observed values from −12 °C to −2 °C. It should be noted that the BRAMS default ice nucleation parameterization (S5) does not allow nucleation warmer than −8 °C.

2.2 Cloud electrification: total flash estimated from precipitable and non-precipitable ice mass fluxes

The main cloud electrification process is based on electrical charge transfer between ice particles during the rebounding collision in the presence of supercooled droplets (MacGorman and Rust, 1998). The amount of charge transferred during each collision is proportional to the size difference between the ice particles, the temperature inside the cloud, and cloud updraft (Takahashi, 1978; Saunders et al., 1991, 2006; Pereyra et al., 2000; Takahashi and Miawaki, 2002). Therefore, the "charging zone" is the zone where graupel/hail and other ice crystal particles, as well as supercooled droplets, coexist.

Based on the charging zone concept, several studies have shown strong correlation between the total (intra-cloud and cloud-to-ground lightning) flash rate and the precipitable and non-precipitable ice mass fluxes (Barthe et al., 2007; Deierling et al., 2008). Deierling et al. (2008) and Barthe et al. (2007) have shown that thunderstorms over Northern Alabama and Oklahoma have a linear relationship between total lightning

ACPD
11, 26143–26171, 2011

flash (cloud-to-ground and intra-cloud together, F, flashes per minute) and the product of the precipitable (f_P, $\mathrm{kg\,m\,s^{-1}}$) and non-precipitable (f_{NP}, $\mathrm{kg\,s^{-1}}$) ice mass fluxes of the type:

$$F = C \cdot f_P \cdot f_{NP} \tag{1}$$

where C ($\mathrm{s\,fl^{-1}\,kg^{-2}\,m^{-1}}$) is a constant, and Deierling et al. (2008) found that $C = 9.0 \times 10^{-15}\,\mathrm{s\,fl^{-1}\,kg^{-2}\,m^{-1}}$, and Barthe et al. (2007) found $C = 1.13 \times 10^{-15}\,\mathrm{s\,fl^{-1}\,kg^{-2}\,m^{-1}}$. f_P is the product of the precipitable ice mass (m_P) and the terminal fall speed of precipitable hydrometeors (v_t),

$$f_P = m_P v_t \tag{2}$$

and f_{NP} is the product of non-precipitable ice mass (m_{NP}) and the vertical change in the updraft velocity w, or the horizontal divergence through the anelastic continuity equation $\nabla_H \rho_0 V = \partial(w\rho_0)/\partial z$),

$$f_{NP} = m_{NP}\partial w/\partial z = m_{NP}(\nabla_H \rho_0 V) \tag{3}$$

In our simulation with BRAMS we can estimate the total flash produced for each individual convective cell by estimating f_P and f_{NP} at each time step. The precipitable hydrometeors in BRAMS are hail and graupel, and the rest of ice species are non-precipitable, i.e. aggregates, snow, and pristine. Therefore, at each time step hail mass and graupel mass were multiplied by their respective terminal fall speed in each grid point and then summed over the storm volume to obtain f_P.

Analogously, the sum of aggregates, snow and pristine masses were multiplied by the horizontal divergence in each grid point and then summed over the storm volume to obtain f_{NP}. Only grid points inside the storm updraft were considered ($w > 0\,\mathrm{m\,s^{-1}}$) and above the level of $-5\,^{\circ}$C, and in the case of f_{NP}, only the ice particles where their terminal fall speed was smaller than the updraft were considered (Barthe et al., 2007; Deierling et al., 2008). Considering C from Deierling et al. (2008) ($C = 9.0 \times 10^{-15}\,\mathrm{s\,fl^{-1}\,kg^{-2}\,m^{-1}}$), we calculated the number of flashes produced in each time step based on Eq. (1). The results are presented in Sect. 3.2.

ACPD
11, 26143–26171, 2011

3 Results and discussions

3.1 Impact on cloud properties and precipitation

Firstly, numerical modeling results are summarized in Table 2 using BRAMS with different IN concentrations as explained in Sect. 2.1. This table shows the total mixing ratio for all types of hydrometeors found for the different simulations indicated in Table 1, as well as the total precipitation at ground level. These values were obtained by integrating the variables in space (vertical and horizontal) and time. It can be seen in Table 1 that the inclusion of IN caused a small impact in total liquid water (cloud water and rain) among the simulations. The simulation with no IN (S1) produced 41 922 $g\,kg^{-1}$ of cloud water and 9092 $g\,kg^{-1}$ rain, less than a unit of percentage from those with IN (S2, S3, S4, S5) for cloud water and a few units of percentage for rain. Among the simulations with IN, only S4 and S6 presented a tendency to decrease the total cloud water, and all those with IN presented a tendency to decrease the total amount of rain at the ground (−8 %). The last result agrees with Levin et al. (2005) with rain reduction at the ground.

However, the impact on the total ice production is very significant. The simulations with *P. syringae* as ice nuclei (S2, S3, S4) produced total hail mixing ratio on the order of 750 $g\,kg^{-1}$ which is ∼100 % greater than the one produced by S1 (380 $g\,kg^{-1}$). The default BRAMS simulation (S5) also produced more hail than the S1 simulation (544 $g\,kg^{-1}$, 43 % more). The simulation with a lower concentration of *P. syringae* (S2) generated 675 % more graupel than S1, and 555 % more than S5. The simulation with an intermediate concentration of *P. syringae* (S3) was the one that produced more snow, and the simulation with the maximum amount of *P. syringae* (S4) produced many more aggregates and ice crystals (565 $g\,kg^{-1}$ and 230 $g\,kg^{-1}$, respectively) than S1 (41 $g\,kg^{-1}$ and 43 $g\,kg^{-1}$, respectively) and the other simulations. More aggregates and ice crystals, as well as graupel and hail, are essential for rebounding ice collisions and therefore for electrical charge transfer and lightning production, as described in the next section (Sect. 3.2).

Discussion Paper | Discussion Paper | Discussion Paper | Discussion Paper |

ACPD

11, 26143–26171, 2011

Effect of bacterial ice nuclei on lightning activity inferred by BRAMS

F. L. T. Gonçalves et al.

To show the temporal evolution of the ice hydrometeors of each simulation, Fig. 3 shows the total mixing ratio of hail, graupel, aggregates, snow and ice crystals for each simulation, integrated over the horizontal and vertical extents of the cloud at each 2-min time step. As shown in Table 2, Fig. 3 also shows that there are significant differences in total hydrometeor mixing ratios among the simulations with no IN (S1) and those with IN (S2, S3, S4, S5), but with temporal details. Table 3 gives the maximums of Fig. 3 and the time when these maximums occurred. The direct impact of IN is on the concentration of pristine ice crystals, which indirectly then impact the production of other hydrometeors. Therefore, S1 simulation produced the fewest ice hydrometeors of all the simulations as no IN were available for nucleation and the only source of ice crystals was due to homogeneous nucleation. This feature also affected the temporal evolution of the cloud: S1 produced significant amounts of frozen hydrometeors (mixing ratios greater than 2 g kg^{-1}) several minutes later than the other ones, as shown in Fig. 3. Ice crystals by homogeneous freezing in S1 had its peak (4.3 g kg^{-1}) at ~10.5 km altitude after 50 min of simulation. The altitude of the peak of ice crystal production was constant in all other simulations and the time when the peak occurred was 2–6 min earlier, except for S3 which occurred at the same time as in S1. The addition of IN tended to generate two peaks of ice crystals: the one at 10.5 km by homogeneous nucleation, and a second one at ~9 km due to heterogeneous nucleation. In simulations S2 and S5 this second peak is not apparent but an elongated branch of 2 g kg^{-1} of ice crystals is observed downward of 10 km after 42 to 48 min of simulation in S2 to S5. In S3 and S4 a second peak of ~4 g kg^{-1} and ~12 g kg^{-1}, respectively, clearly developed at $t = 44$ min due to more IN.

Greater amounts of ice crystals in S2 to S5 impacted the production of other ice species, first due to rimming and accretion generating greater amounts of aggregates (>2 g kg^{-1}) as soon as 40 min of simulation for S3 and S4, and 2 min later for S2 and S5. Aggregates also presented two peaks in S2 to S5, at the same heights as the ice crystal peaks due to the conversion of ice crystals into aggregates by rimming, accreation and auto-conversion. S5 presented the highest aggregate peak with 33 g kg^{-1} at

$t = 48$ min. Snow also presented the same behavior in time and vertical space as aggregates: maximums of snow were produced at ~9 and 10.5 km of height also due to rimming, accretion and auto-conversion of ice crystals, except for S5 which presented a single peak at ~9 km of half (5.7 g kg^{-1}) of the intensity of the other IN simulations (~13 g kg^{-1}). This behavior might be because ice crystals would accreate and rime in higher rates, as well as auto-convert, in an environment with greater amounts of ice crystals, forming aggregates more quicker than in environments with fewer ice crystals.

The behavior of ice crystals, snow, and aggregates described above was also translated into greater amounts of hail and graupel. S1 resulted in a hail maximum of 15 g kg^{-1} at $t = 46$ min, and a graupel maximum of only 1.2 g kg^{-1} at $t = 48$ min, while the bacterial simulations (S2, S3, S4) produced three times more hail (~45 g kg^{-1}) 8 min earlier (Table 3 and Fig. 3). The production of graupel by S2, S3 and S4 was also higher than in S1 but decreased as the *P. syringae* concentration increased, giving place to the production of aggregates. The aggregates increased as the *P. syringae* concentration increased with a maximum of 33 g kg^{-1} at $t = 48$ min for S4, 22 g kg^{-1} at $t = 48$ min, and 18 g kg^{-1} at $t = 46$ min, as shown in Table 3 and Fig. 3.

Scenario S6, presenting the BRAMS default scenario (S5) plus S4 (the highest bacteria concentration), displays similar scenario of S4. Some of the hydrometeors presents even higher concentrations (see Table 2), compared to the previous simulations. However, the precipitable ice shows a decrease of less than 5 % compared to S4 simulation. Therefore, it can be inferred from the above results that even a smaller concentrations of IN, at warmer temperatures, would accelerate the process of generation of hail and aggregates. This acceleration would be due to higher rates of accreation and rimming, and then auto-conversion, which quickly transform graupel and snow into hail and aggregates (respectively), decreasing the amount of graupel and snow inside the cloud. The next section shows how these changes in ice species affect cloud electrification.

ACPD
11, 26143–26171, 2011

3.2 Impact on cloud electrification

As shown in Sect. 2.2, the amount of precipitable ice (graupel and hail) and non-precipitable ice (aggregates, snow and ice crystals) are key ingredients for cloud electrification and lightning production. Table 2 shows that *P. syringae* simulations produced greater amounts of both total precipitable and non-precipitable ice than S1 and S5. The highest total precipitable ice mixing ratio was observed in S3 with 940 g kg^{-1}, but the other IN simulations had comparable values. In the case of total non-precipitable mass, S4 produced the greatest amount (886 g kg^{-1}), followed by S3, S2, and then S5, with not so comparable values (717, 601, and 506 g kg^{-1}, respectively).

However, the strength of the updraft also controls cloud electrification. Stronger updrafts can happen at the same time as high generation of precipitable and non-precipitable ice to efficiently promote rebounding collisions between these species to transfer electrical charges. Therefore, Fig. 3 shows the precipitable ice mass flux (f_P), non-precipitable ice mass flux (f_{NP}) and maximum cloud updraft (w) at each 2-min time step for each of the simulations, Also, Table 4 shows the maximum value of these variables during the whole simulation. It can be seen that simulations with IN developed stronger updrafts, with the one with more ice production (S4), and therefore greater latent heat release, having the stronger w: 25.2 m s^{-1}. Therefore, the estimated lightning flash rate described in Sect. 2.2 revealed 6 flashes for S5, and none for S1.

It can be seen that the simulation with no ice nuclei (S1) did not produce lighting because of the very small production of non-precipitable ice mass flux, 6×10^3 kg s^{-1} (Fig. 4 and Table 3), compared to IN simulations that produced 3 orders of magnitude greater than S1. The low production of f_{NP} led to a low production of precipitable ice particles (e.g. graupel and hail) by rimming and auto-conversion processes as shown in Sect. 3.1. This implied a 36 % smaller f_P in S1 (5.04×10^8 kg m s^{-1}) than the control run (S5, BRAMS default) (7.92×10^8 kg m s^{-1}), as the maximum updrafts are similar in S1 and S5 (Fig. 3 and Table 4). When *P. syringae* ice nuclei were included in S2, S3, S4 the production of ice crystals increased as well, generating 4, 5 and 6 flashes,

ACPD
11, 26143–26171, 2011

respectively. S6 simulation, although, presents same amount of flash of S4, six flashes in total (Table 3). Consequently, the high number of IN, from BRAMS default, acting below $-10\,^{\circ}$C, plays a secondary role at all.

4 Conclusions

The results of this work suggest that in clouds, the presence of biological ice nuclei active at relatively warm temperatures, and in particular the bacterium *P. syringae*, induces an increase in cloud ice which in turn induces an increase of cloud electricity. It must be clarified, that these simulations deal with small clouds with short life and involve very simple numerical modeling. Therefore, the results of this simple numerical modeling emphasize that biological IN or IN with warm temperature activity (warmer than $-10\,^{\circ}$C) are relevant to cloud electricity, as has been suggested previously in the work of Phillips et al. (2009). BRAMS default IN concentration seems to play a secondary role at all, not affecting the total number of flashes, when both simulation (with bacteria IN concentration and default) are acting together. These authors found that INA can influence significantly the average numbers and sizes of crystals in the clouds; the horizontal cloud coverage, precipitation and incident solar insolation at the surface and they open questions about whether emissions of INA particles can be modified by their own effects on clouds and atmospheric conditions. Future simulations could explore deeper convective storms in other realistic contexts that involve more detailed parameterization of the hydrometeor concentrations.

The real biological IN activity inside of clouds is a rather unknown factor with many implications, including for cloud tops, rainfall amount and cloud albedo as examples, as emphasized by Phillips et al. (2009) article. Additionally, there are many other biological materials acting as IN such as, fungal spores, algae, pollen, other bacterial species, etc. (Morris et al., 2004; Pouleur et al., 1992), when taken together may have an even more important potential impact on cloud parameters and cloud electricity. Additionally, cloud electrification, by itself, has many important impacts, among them, public security.

ACPD
11, 26143–26171, 2011

Acknowledgements. We thank the Ohrstrom Foundation, Inc. for a generous donation to fund research meetings between the first and last author leading to the conception and realization of this work.

References

Amato, P., Menager, M., Sancelme, M., Laj, P., Mailhot, G., and Delort, A.-M.: Microbial population in cloud water at the Puy de Dôme. Implications for the chemistry of clouds, Atmos. Environ., 39, 4143–4153, 2005.

Amato, P., Parazols, M., Sancelme, M., Laj, P., Mailhot, G., and Delort, A.-M.: Microorganisms isolated from the water phase of tropospheric clouds at the Puy de Dôme: major groups and growth abilities at low temperatures, FEMS-Microbiol. Ecol., 49(2), 242–254, doi:10.1111/j.1574-6941.2006.00199, 2007.

Ariya, P. A. and Amyot, M.: New directions: The role of bioaerosols in atmospheric chemistry and physics, Atmos. Environ., 38, 1231–1232, 2004.

Barthe, C., Deirling, E., and Barth, M. C.: On the use of ice mass fluxes to estimate total lightning in cloud resolving modes, EOS Trans. AGU, 88(52), Fall Meeting Suppl., Abstract AE43A-02, 2007.

Bauer, H., Giebl, H., Hitzenberger, R., Kasper-Giebl, A., Reischl, G., Zibuschka, F., and Puxbaum, H.: Airborne bacteria as cloudcondensation nuclei, J. Geophys. Res., 108, AAC2/1–AAC2/5, 2003.

Christner, B. C., Morris, C. E., Foreman, C. M., Cai, R., and Sands, D. C.: Ubiquity of biological ice nucleators in snowfall, Science, 319, 1214, doi:10.1126/science.1149757, 2008.

Cotton, W. R., Tripoli, G. J., Rauber, R. M., and Mulvihill, E. A.: Numerical simulation of the effects of varying ice crystal nucleation rates and aggregation processes on orographic snowfall, J. Climate Appl. Meteorol., 25, 1668–1680, 1986.

Deierling, W., Petersen, W. A., Latham, J., Ellis, S., and Christian, H. J.: The relationship between lightning activity and ice fluxes in thunderstorms, J. Geophys. Res., 113, D15210, doi:10.1029/2007JD009700, 2008.

Deguillaume, L., Leriche, M., Amato, P., Ariya, P. A., Delort, A.-M., Pöschl, U., Chaumerliac, N., Bauer, H., Flossmann, A. I., and Morris, C. E.: Microbiology and atmospheric pro-

ACPD
11, 26143–26171, 2011

cesses: chemical interactions of primary biological aerosols, Biogeosciences, 5, 1073–1084, doi:10.5194/bg-5-1073-2008, 2008.

DeMott, P. J., Meyers, M. P., and Cotton, W. R.: Parameterization and impact of ice initiation 755 processes relevant to numerical model simulations of cirrus clouds, J. Atmos. Sci., 51, 77–90, 1994.

Diehl, K., Matthias-Maser S., Mitra, S. K., and Jaenicke R.: Laboratory studies on the ice nucleating ability of biological aerosol particles in condensation freezing, immersion freezing and contact freezing modes, J. Aerosol Sci., 31, S70–S71, 2000.

Elbert, W., Taylor, P. E., Andreae, M. O., and Pöschl, U.: Contribution of fungi to primary biogenic aerosols in the atmosphere: wet and dry discharged spores, carbohydrates, and inorganic ions, Atmos. Chem. Phys., 7, 4569–4588, doi:10.5194/acp-7-4569-2007, 2007.

Freitas, S. R., Longo, K. M., Silva Dias, M. A. F., Chatfield, R., Silva Dias, P., Artaxo, P., Andreae, M. O., Grell, G., Rodrigues, L. F., Fazenda, A., and Panetta, J.: The Coupled Aerosol and Tracer Transport model to the Brazilian developments on the Regional Atmospheric Modeling System (CATT-BRAMS) – Part 1: Model description and evaluation, Atmos. Chem. Phys., 9, 2843–2861, doi:10.5194/acp-9-2843-2009, 2009.

Gonçalves, F. L. T., Martins, J. A., and Silva Dias, M. A. F.: Shape parameter analysis using cloud spectra and gamma functions in the numerical modeling RAMS during LBA Project at Amazonian region, Brazil, Atmos. Res., 89(1–2), 1–11, http://www.sciencedirect.com/science/journal/01698095, 2008.

Hamilton, W. D. and Lenton, T. M.: Spora and Gaia: how microbes fly with their clouds, Ethology, Ecology and Evolution, 10, 1–16, 1998.

Hoose, C., Kristjánsson, J. E., and Burrows, S. M.: How important is biological ice nucleation in clouds on a global scale?, Environ. Res. Lett., 5, 024009, doi:10.1088/1748-9326/5/2/024009, 2010.

Jaenicke, R.: Abundance of cellular material and proteins in the atmosphere, Science, 308, 5718, doi:10.1126/science.1106335, 2005.

Levin, Z., Teller, A., Ganor, E., and Yin, Y.: On the interactions of mineral dust, sea-salt particles, and clouds: A measurement and modeling study from the Mediterranean Israel Dust Experiment campaign, J. Geophys. Res., 110, D20202, doi:10.1029/2005JD005810, 2005.

Martins, J. A. and Silva Dias, M. A. F.: The impact of smoke from forest fires on the spectral dispersion of cloud droplet size distributions in the Amazonian region, Environ. Res. Lett., 4, 015002, doi:10.1088/1748-9326/4/1/015002, 2009.

ACPD
11, 26143–26171, 2011
Effect of bacterial ice nuclei on lightning activity inferred by BRAMS
F. L. T. Gonçalves et al.

Martins, J. A., Silva Dias, M. A. F., and Gonçalves, F. L. T.: Impact of biomass burning aerosols on precipitation in the Amazon: A modeling case study, J. Geophys. Res., 114, 1–68, 2009.
MacGorman, D. R. and Rust, W. D.: The electrical nature of storms, Oxford University Press, New York, 422 pp., 1998.
Meyers, M. P., Walko, R. L., Harrington, J. Y., and Cotton, W. R.: New RAMS cloud microphysics parameterization. Part II: The two-moment scheme, Atmos. Res., 45, 3–39, 1997.
Möhler, O., DeMott, P. J., Vali, G., and Levin, Z.: Microbiology and atmospheric processes: the role of biological particles in cloud physics, Biogeosciences, 4, 1059–1071, doi:10.5194/bg-4-1059-2007, 2007.
Möhler, O., Georgakopoulos, D. G., Morris, C. E., Benz, S., Ebert, V., Hunsmann, S., Saathoff, H., Schnaiter, M., and Wagner, R.: Heterogeneous ice nucleation activity of bacteria: new laboratory experiments at simulated cloud conditions, Biogeosciences, 5, 1425–1435, doi:10.5194/bg-5-1425-2008, 2008.
Morris, C. E., Georgakapoulos, D., and Sands, D. C.: Ice nucleation active bacteria and their potential role in precipitation, J. Phys. IV, France, 121, 87–103, 2004.
Morris, C. E., Sands, D. C., Vinatzer, B. A., Glaux, C., Guilbaud, C., Buffière, A., Yan, S., Dominguez, H., and Thompson, B. M.: The life history of the plant pathogen *Pseudomonas syringae* is linked to the water cycle, ISME Journal, 2, 321–334, 2008.
Morris, C. E., Sands, D. C., Vanneste, J. L., Montarry, J., Oakley, B., Guilbaud, C., and Glaux, C.: Inferring the evolutionary history of the plant pathogen *Pseudomonas syringae* from its biogeography in headwaters of rivers in North America, Europe and New Zealand, *mBio*, 1(3), e00107-10–e00107-20, 2010.
Morris, C. E., Sands, D. C., Bardin, M., Jaenicke, R., Vogel, B., Leyronas, C., Ariya, P. A., and Psenner, R.: Microbiology and atmospheric processes: research challenges concerning the impact of airborne micro-organisms on the atmosphere and climate, Biogeosciences, 8, 17–25, doi:10.5194/bg-8-17-2011, 2011.
Orser, C., Staskawicz, B. J., Panopoulos, N. J., Dahlbeck, D., and Lindow, S. E.: Cloning and expression of bacterial ice nucleation genes in *Escherichia coli*, J. Bacteriol., 184, 359–366, 1985.
Pereyra, R. G., Avila, E. E., Castellano, N. E., and Saunders, C.: A laboratory study of graupel charging, J. Geophys. Res., 105, 20803–20812, 2000.
Phillips, V. T. J., Andronache, C., Christner, B., Morris, C. E., Sands, D. C., Bansemer, A., Lauer, A., McNaughton, C., and Seman, C.: Potential impacts from biological aerosols

ACPD
11, 26143–26171, 2011

Effect of bacterial ice nuclei on lightning activity inferred by BRAMS

F. L. T. Gonçalves et al.

on ensembles of continental clouds simulated numerically, Biogeosciences, 6, 987–1014, doi:10.5194/bg-6-987-2009, 2009.

Pouleur, S., Richard, C., Martin, J. G., and Antoun, H.: Ice Nucleation Activity in *Fusarium acuminatum* and *Fusarium avenaceum App. Environ. Microbiol*, 58, 2960–2964, 1992.

Sands, D. C., Langhans, V. E., Scharen, A. L., and de Smet, G.: The association between bacteria and rain and possible resultant meteorological implications, J. Hungarian Meteorol. Serv., 86, 148–152, 1982.

Saunders, C. P. R., Keith, W. D., and Mitzeva, R. P.: The effect of liquid water on thunderstorm charging, J. Geophys. Res., 96, 11007–11017, 1991.

Saunders, C. P. R., Bax-Norman, H., Emersic, C., Avila, E. E., and Castellano, N. E.: Laboratory studies of the effect of cloud conditions on graupel/crystal charge transfer in thunderstorm electrification, Q. J. Roy. Meteorol. Soc., 132, 2653–2673, doi:10/1256/qj.05.218, 2006.

Sattler, B., Psenner R., Puxbaum, H., and Limbeck, A.: Clouds as habitat and seeders of active bacteria. Proc. SPIE – The International Society for Optical Engineering 4495 (Instruments, Methods, and Missions for Astrobiology IV), 211–222, 2002.

Sattler, B., Puxbaum, H., and Psenner, R. Bacterial growth in supercooled cloud droplets, Geophys. Res. Lett., 28, 239–242, 2001.

Szyrmer, W. and Zawadzki, I.: Biogenic and anthropogenic sources of ice-forming nuclei: A review, B. Am. Meteorol. Soc., 78, 209–228, 1997.

Takahashi, T.: Riming electrification as a charge generation mechanism in thunderstorms, J. Atmos. Sci., 35, 1536–1548, 1978.

Takahashi, T. and Miyawaki, K.: Reexamination of riming electrification in a wind tunnel, J. Atmos. Sci., 59, 1018–1025, 2002.

Tripoli, G. J. and Cotton, W. R.: The Colorado State University three-dimensional cloud mesoscale model, Part I: General theoretical framework and sensitivity experiments, J. Rech. Atmos., 16, 185–220, 1982.

Walko, R., Cotton, W. R., Meyers, M. P., and Harrington, J. Y.: New RAMS cloud microphysics parameterization. Part I: The single-moment scheme, Atmos. Res., 38, 29–62, 1995.

Table 1. Type of nucleation considered in each simulation.

Type of ice nucleation/Simulation	Homogeneous	Deposition	Condensation and Freezing	Contact and Freezing	Bacterial-concentrations
S1	Yes	No	No	No	No
S2	Yes	No	No	No	Yes, $w/10^3\ l^{-1}$
S3	Yes	No	No	No	Yes, $w/10^4\ l^{-1}$
S4	Yes	No	No	No	Yes, $w/10^5\ l^{-1}$
S5	Yes	Yes	Yes	Yes	No
S6	Yes	Yes	Yes	Yes	Yes, $w/10^5\ l^{-1}$

ACPD
11, 26143–26171, 2011

Table 2. Total mixing ratio ($g\,kg^{-1}$) of hydrometeors for all simulations. These values were obtained by summing the variables in the entire domain (horizontal and vertical) and duration (3 h) of the simulations. Values in parentheses are the percentage deviation from the simulation with no IN (S1, i.e. percentage deviation = $v_{Sy}/v_{S1} \cdot 100\,\%–100\,\%$, where v is the variable and y is the simulation type).

	S1	S2	S3	S4	S5	S6
Cloud water	41 922	42 066 (+0.3 %)	41 965 (+0.1 %)	41 645 (−0.7 %)	42 085 (+0.4 %)	41 453 (−1.1 %)
Rain	9092	8398 (−8 %)	8370 (−8 %)	8320 (−8 %)	8618 (−5 %)	8355 (−8 %)
Hail	380	752 (+98 %)	775 (+104 %)	758 (+100 %)	544 (+43 %)	774 (+104 %)
Graupel	29	225 (+675 %)	164 (+465 %)	88 (+203 %)	190 (+555 %)	149 (+414 %)
Aggregates	41	308 (+644 %)	372 (798 %)	565 (+1265 %)	223 (+437 %)	465 (+1022 %)
Snow	68	210 (+211 %)	235 (+248 %)	90 (+34 %)	199 (+194 %)	210 (+210 %)
Ice crystal	43	83 (+93 %)	110 (+155 %)	230 (+433 %)	85 (+96 %)	107 (+147 %)
Precipitable ice	409	977 (+139 %)	940 (+130 %)	846 (+107 %)	734 (+80 %)	924 (+126 %)
Non-precipitable ice	152	601 (+295 %)	717 (+371 %)	886 (+482 %)	506 (+233 %)	781 (+413 %)

ACPD
11, 26143–26171, 2011

ACPD
11, 26143–26171, 2011

Effect of bacterial ice nuclei on lightning activity inferred by BRAMS

F. L. T. Gonçalves et al.

Table 3. Maximum of ice hydrometeor mixing ratio for each simulation, where the values in parentheses are the time in minutes when the maximum occurred.

	S1	S2	S3	S4	S5	S6
Hail	15 ($t = 6$)	42 ($t = 40$)	46 ($t = 40$)	47 ($t = 40$)	26 ($t = 42$)	46 ($t = 40$)
Graupel	1.2 ($t = 48$)	10 ($t = 46$)	6.8 ($t = 46$)	3.2 ($t = 46$)	9.2 ($t = 46$)	6.6 ($t = 44$)
Aggregates	3.6 ($t = 52$)	18 ($t = 46$)	22 ($t = 48$)	33 ($t = 48$)	13 ($t = 46$)	26 ($t = 48$)
Snow	2.9 ($t = 58$)	12 ($t = 46$)	14 ($t = 48$)	5.5 ($t = 44$)	13 ($t = 46$)	12 ($t = 46$)
Ice Crystal	4.3 ($t = 50$)	5.1 ($t = 48$)	4.7 ($t = 50$)	13 ($t = 44$)	4.6 ($t = 48$)	4.4 ($t = 48$)

Table 4. Maximum precipitable ice mass flux (f_P), non-precipitable ice mass flux (f_{NP}), and cloud updraft (w), as well as the total estimated number of lightning flashes for each simulation. Numbers in parentheses indicate the time step when the maximum occurred.

	maximum f_P (kg m s^{-1})	maximum f_{NP} (kg s^{-1})	maximum w (m s^{-1})	Total estimated lightning flashes
S1	5.04×10^8 (t=46*)	0.065×10^5 (t=46*)	19.1 (t=40*)	0
S2	8.86×10^8 (t=44)	1.27×10^5 (t=44)	23.6 (t=44)	4
S3	8.60×10^8 (t=44)	1.62×10^5 (t=44)	24.1 (t=44)	5
S4	8.14×10^8 (t=42)	2.11×10^5 (t=44)	25.2 (t=45)	6
S5	7.92×10^8 (t=42)	0.925×10^5 (t=44)	21.5 (t=44)	3
S6	9.08×10^8 (t=42)	2.08×10^5 (t=44)	25.5 (t=42)	6

* All time steps are given in minutes.

ACPD
11, 26143–26171, 2011
Effect of bacterial ice nuclei on lightning activity inferred by BRAMS
F. L. T. Gonçalves et al.

Fig. 1a. Study area where the radiosonde was launched.

ACPD
11, 26143–26171, 2011

Effect of bacterial ice nuclei on lightning activity inferred by BRAMS

F. L. T. Gonçalves et al.

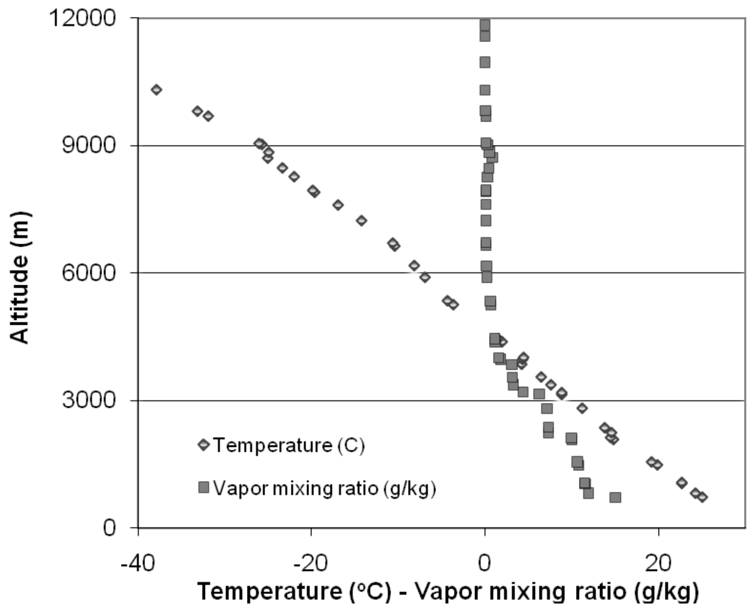

Fig. 1b. Radiosonde of 3 March 2003 at São Paulo airport (12:00 GMT), with temperature (°C) and vapor ratio (g kg^{-1}) vertical profiles.

ACPD
11, 26143–26171, 2011

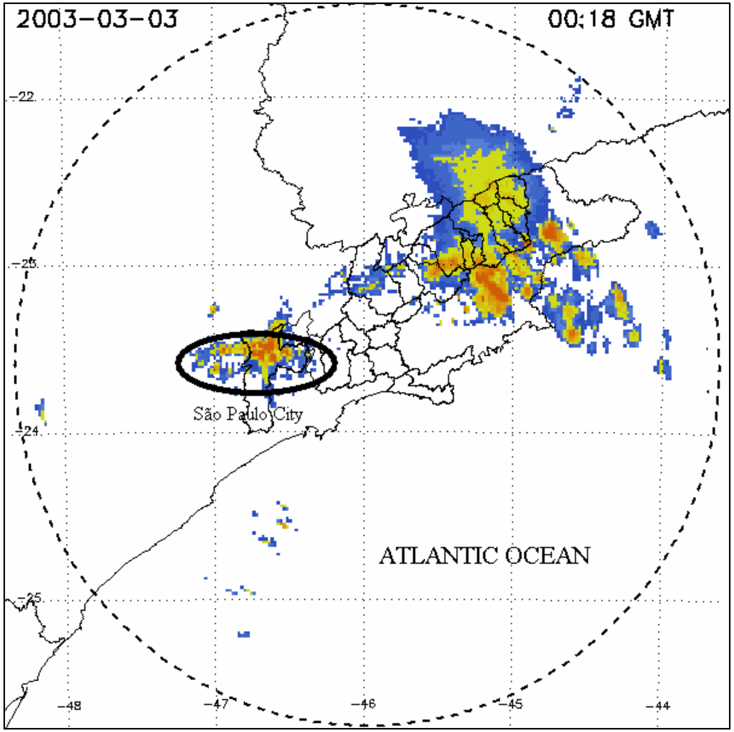

Fig. 1c. 3 March 2003 radar data at 18:00 GMT. Bluish and greenish colors mean 30 dBz or less, or less than 5 mm h^{-1}. Orange and reddish colors mean more than 40 dBz and more than 20 mm h^{-1}. The circled area correspond to the study area.

ACPD
11, 26143–26171, 2011

Title Page
Abstract | Introduction
Conclusions | References
Tables | Figures
◂| |▸
◂ ▸
Back | Close
Full Screen / Esc
Printer-friendly Version
Interactive Discussion

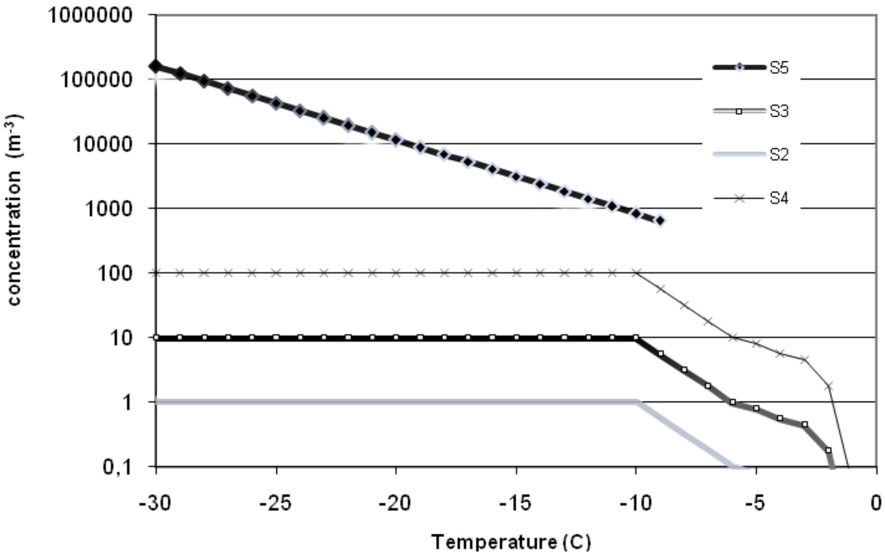

Fig. 2. Ice nuclei concentration profiles (m^{-3}), where 10 bacteria per m^3 corresponds to 1000 IN bacteria per L of cloud water (S3 scenario), for different numerical scenarios involving the bacterium *P. syringae* (S2, S3, S4) and BRAMS default parameterization (S5). Scenario S6 is performed summing up S4 and S5.

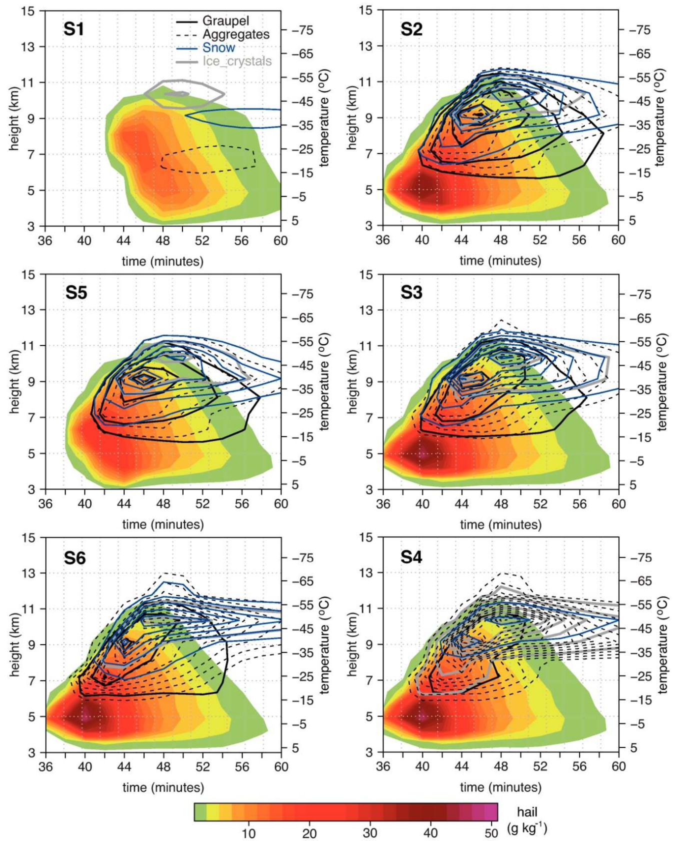

Fig. 3. Total mixing ratio of ice hydrometeors (hail – shadded, and graupel, aggregates, snow and ice crystals – contours) for each simulation. Values are integrated over the horizontal and vertical extents of the cloud at each 2-min time step. Contour lines are mixing ratios for every $2\,\mathrm{g\,kg^{-1}}$.

ACPD
11, 26143–26171, 2011

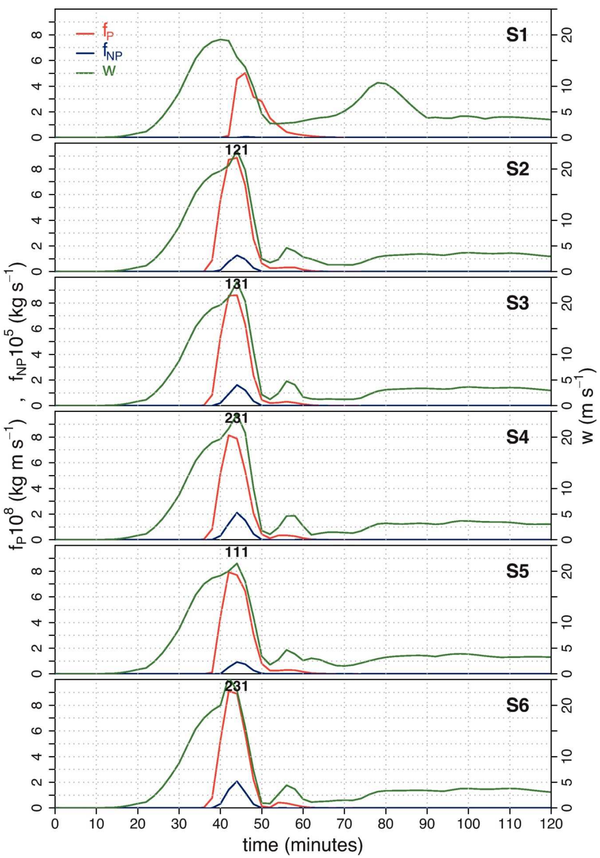

Fig. 4. Precipitable ice mass flux (f_P), non-precipitable ice mass flux (f_{NP}) and maximum cloud updraft (w) at each time step for each simulation. Numbers at the top of each panel correspond to the estimated lighting flashes individually at the respective time step. The total flash number corresponds to the sum of those numbers, for example, "231" means $2+3+1=6$, and therefore, at scenario S4 and S6, the total flash number was 6.

ACPD
11, 26143–26171, 2011

Effect of bacterial ice nuclei on lightning activity inferred by BRAMS

F. L. T. Gonçalves et al.